International Journal of Oil, Gas and Coal Engineering
2025, Vol. 13, No. 1, pp. 1-14
https://doi.org/10.11648/j.ogce.20251301.11

Research Article

Research on Roadway Surrounding Rock Migration and Gob-side Entry Support Techniques in Top Coal Caving of Steeply Inclined Coal Seams with a Single Roadway

Kangzhan Ding[1], Zhaowen Du[1,*], Zongbin Ma[2], Jiandu Su[2], Zhongping Guo[1]

[1]School of Energy and Mining Engineering, Shandong University of Science and Technology, Qingdao, China
[2]Jingtai Coal Industry Company Limited, Baiyin, China

Abstract

The "single roadway top coal mining method for steep and medium-thick seams" addresses the challenges posed by significant variations in seam dip angles and thicknesses. This approach segments the seam into multiple sections along its incline, with each section utilizing a single roadway aligned with the seam's trend. This roadway is dedicated to one coal mining section, managing the ventilation, transport, and pedestrian traffic for the working face. To ensure the effective execution of this method, numerical simulations are employed to examine the surrounding rock movement after the working face advances. Two roadway preservation techniques are proposed, tailored to different burial depths: the "flexible mold concrete wall" and the "flexible mold concrete wall + right-angle tram I-steel roof." Both methods undergo theoretical analysis and numerical validation. Practical application demonstrates that these techniques effectively stabilize the surrounding rock, prevent airflow between the roadway and the gob, mitigate gas accumulation, and reduce the risk of spontaneous combustion in the residual coal. This method enables efficient single roadway top coal mining and offers crucial technical support for similar roadway support challenges, holding significant theoretical and practical relevance.

Keywords

Gob Retaining Roadway, Flexible Form Concrete, Roadway Side Support, Reinforcing Support

1. Introduction

Maintaining a roadway along the goaf involves preserving the original roadway after coal face advancement, ensuring it remains undamaged and continues to function in coal mining operations. Achieving goaf retention requires selecting appropriate support methods for the goaf-side roadway. Based on the materials used, support methods are classified into wood stack support, masonry gangue belt support, dense support, artificial stack support, and rigid pouring belt support. Retaining the post-mining roadway via goaf retention enables the recovery of coal pillars and preservation of the original roadway, thereby minimizing coal loss and reducing excavation volume, which offers significant economic advantages.

In recent years, substantial research has been conducted on

*Corresponding author: 18764268819@163.com (Zhaowen Du)

Received: 10 December 2024; **Accepted:** 23 December 2024; **Published:** 14 January 2025

gob retention under inclined coal seam mining conditions. He et al. enhanced conventional goaf retention techniques by introducing a method involving roof cutting and pressure relief. Through shaped charge blasting, they pre-cut the roof seam adjacent to the mining roadway, transforming the roof into a sidewall for the retention roadway post-mining (e.g., [1]). Wang investigated the optimal height and angle for roof cutting in gob retention, concluding that cutting through thick hard roof layers yields more pronounced pressure relief effects (e.g., [2]). Zhu et al., using numerical simulation and theoretical calculations, explored the parameters for gob retention lanes under thick hard roof conditions, systematically outlining the key parameter determination method in such scenarios (e.g., [3]). Guo et al., focusing on thick coal seam mining, proposed a "flexible concrete + reinforced support" approach to stabilize surrounding rock during gob retention, Feffectively reducing roof, floor, and side displacement (e.g., [4]). Zhang et al. analyzed the support and stability of soft film concrete retention roadways in shallow coal seams, demonstrating the strong safety performance of soft film concrete as side support in these conditions (e.g., [5]).

Research on gob-retaining methods and parameters predominantly draws from various mechanical models of surrounding rock in gob-retaining conditions. Currently, several models are recognized: He's mechanical model of separated rock blocks (e.g., [6]), Wang's roof tilt mechanical model, Sun's bending moment failure model for rectangular stacked laminae, Li's block balance model (e.g., [7]), and Tu's elastic sheet roof motion model (e.g., [8]). Among these, the separated rock block model is frequently employed to estimate the support load at the gob-retaining lane's side, guiding the determination of support methods and parameters based on these calculations. In cases where "single roadway caving top coal in steep inclined seam" mining is employed, the roadway must be preserved for continued use after the working face advances. However, the absence of a continuous roof over the top coal precludes the application of the separated rock block model, rendering existing gob-retaining roadway models unsuitable for this scenario. The lack of mechanical research tailored to this unique condition underscores the necessity for focused study. This paper addresses the steep coal seam single-roadway top-caving mining method by analyzing the surrounding rock displacement prior to roadway retention, proposing and verifying a retention method to ensure safe production continuity in the coal mining section.

2. Engineering Background

The primary coal seam, designated as seam 8, lies at a depth ranging from 50m to 400m within the planned mining area. Its extraction thickness varies between 1.32m and 3.47m, with an average of 2.91m. The coal seam's dip angle generally falls between 60 °and 65 °, with localized steepness reaching up to 75 °, and its strike exhibits significant variability. The immediate roof consists of 3.1m of fine-grained sandstone, while the main roof comprises 3.4m of siltstone, and the underlying floor features 10.8m of fine-grained sandstone. Based on these geological conditions, the single-roadway top coal caving method was employed for extraction, as illustrated in Figure 1 and Figure 2. This fully mechanized caving method for steeply inclined seams involved dividing the seam into sections along its dip, with each section serviced by a single roadway and a fully mechanized system (e.g., [9]). The designed mining height was set at 3m, while the coal caving height reached 12m, resulting in a mining-to-caving ratio of 1:4. As the face advanced, an "empty wall" formed on one side of the roadway, leaving only one side with a wall, hence the term "single-side roadway." This roadway was maintained along the goaf to provide structural support and isolate the mined-out area, while a new return airway was constructed to facilitate ventilation and worker access.

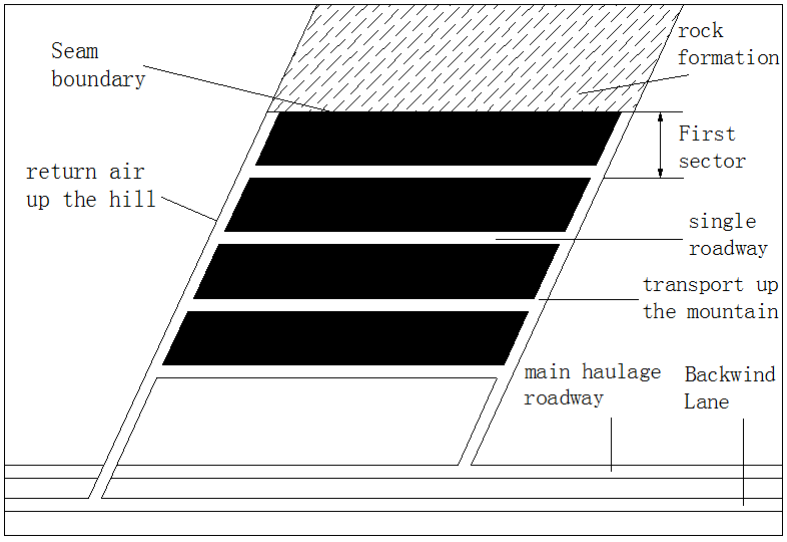

Figure 1. *Figure caption Schematic diagram of the production system for sharply inclined single-roadway mining method.*

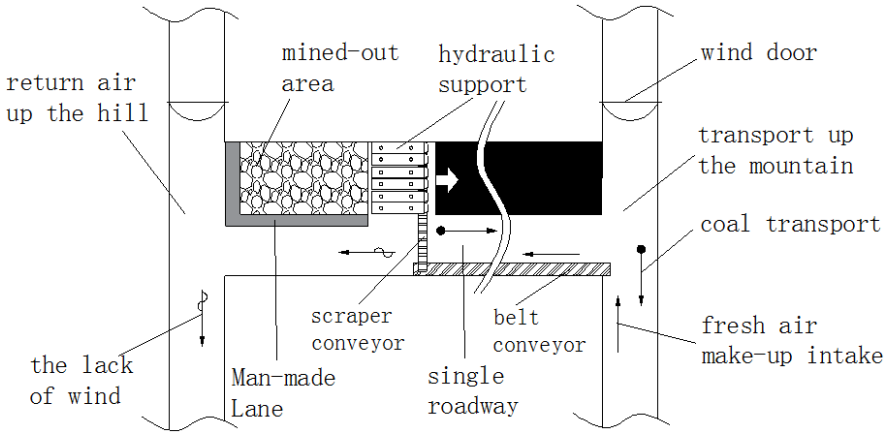

Figure 2. *Schematic diagram of the production system for sharply inclined single-roadway mining method.*

3. Study on Stress-Strain Law of Surrounding Rock of Single-side Roadway

To implement targeted roadway retention maintenance, FLAC3D simulations were conducted on the surrounding rock after the completion of top coal caving, but post-roadway retention maintenance. A Mohr-Coulomb model, representing the geological conditions of the No. 8 coal seam in Baiyanzi mine, was developed. Simulations were performed at varying burial depths of 100m, 200m, 300m, 400m, 500m, 600m, 700m, 800m, 900m, and 1000m. The physical and mechanical parameters of the coal rock strata were detailed in Table 1. The cmodel command was employed to replicate the top coal caving process, enabling a comparative analysis of the stress-strain behavior of the surrounding rock at different burial depths. This approach offers a clearer understanding of the stress-strain responses in varying geological conditions. The investigation focused on the stress-strain patterns within the surrounding rock of a single roadway in a steep coal seam, providing insights to address the challenges in maintaining roadway retention under such conditions.

Table 1. *Physical and mechanical parameters of No. 8 coal and its surrounding rock.*

Rock formation		Shear / GPa	Bulk / GPa	Cohesion / MPa	Internal friction Angle / (°)	Tensile strength /MPa	Density / (kg/m)
Coal seam roof	Fine grained sandstone	1.2	1.0	2.6	37	3.8	2600
	Siltstone	1.7	3.9	2.0	34	2.1	2400
8 coals		0.38	0.65	0.95	32	0.86	1460
Coal seam floor	Siltstone	1.3	2.7	2.2	33	2.6	2400
	Fine grained sandstone	1, 2,	1.5	2.9	34	2.9	2600

3.1. Stress Condition of Surrounding Rock of Single-side Roadway

Figure 3 illustrated the horizontal stress distribution at varying burial depths. With the advancement of the working face, a suspended triangular rock mass emerged above the roadway, resulting in a localized stress concentration zone within. As burial depth increased, the surrounding rock experienced heightened stress levels, leading to a more pronounced concentration of stress.

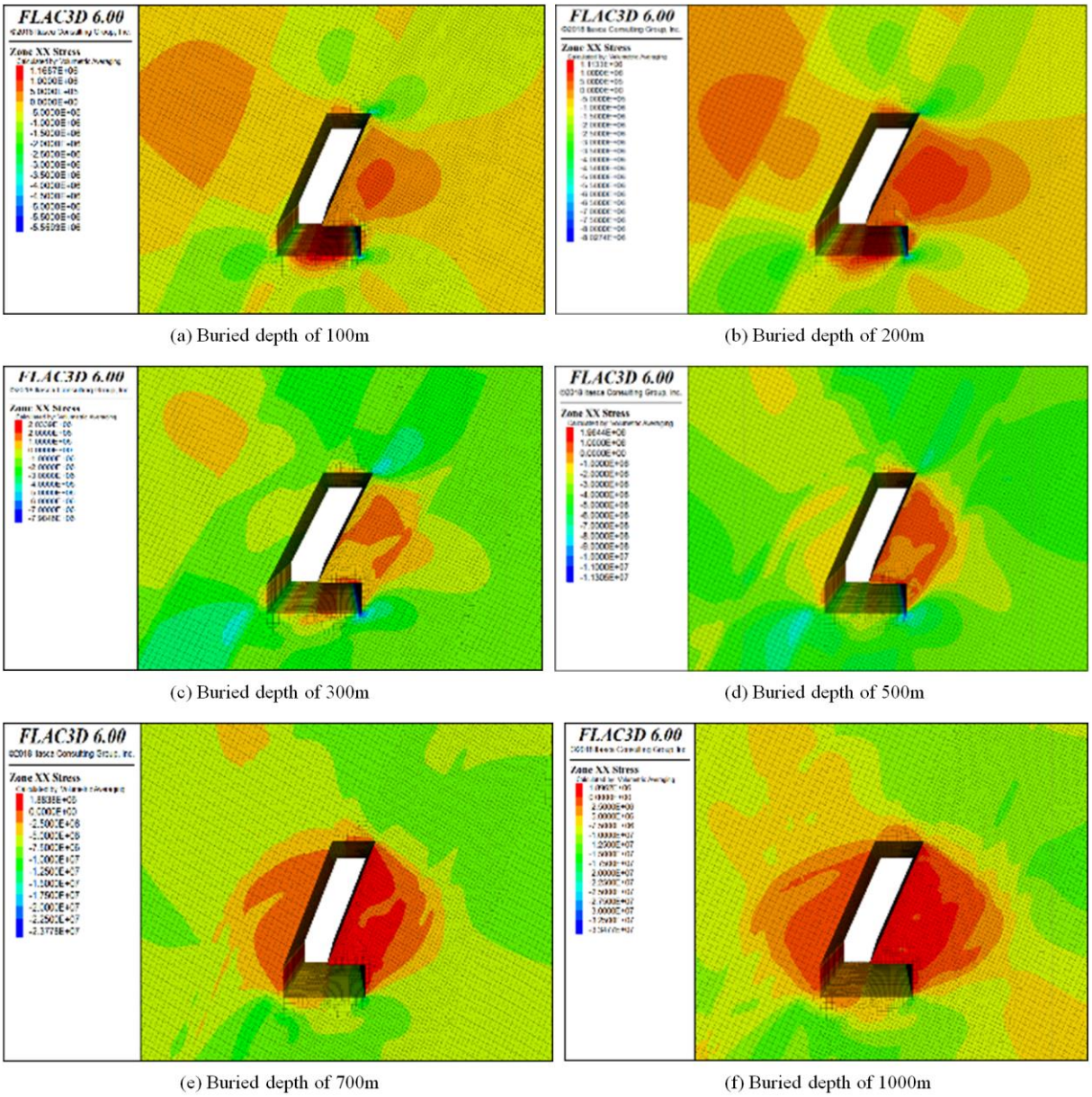

(a) Buried depth of 100m (b) Buried depth of 200m

(c) Buried depth of 300m (d) Buried depth of 500m

(e) Buried depth of 700m (f) Buried depth of 1000m

Figure 3. *Horizontal stress distribution in roadway surrounding rock post-advancement of the working face.*

Figure 4 illustrated the vertical stress distribution at varying burial depths. As the working face progressed, stress concentrations developed within the "triangular" rock mass and the roadway floor. Notably, the degree of stress concentration remained consistent across different burial depths.

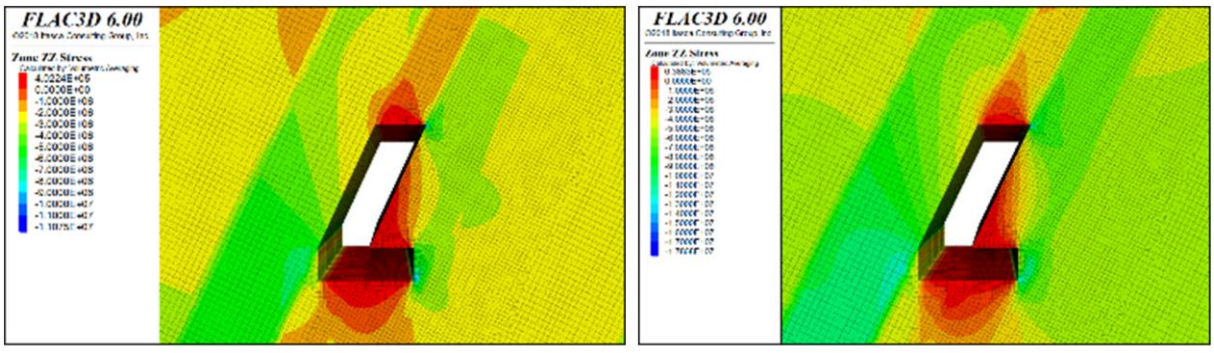

(a) Buried depth of 100m (b) Buried depth of 200m

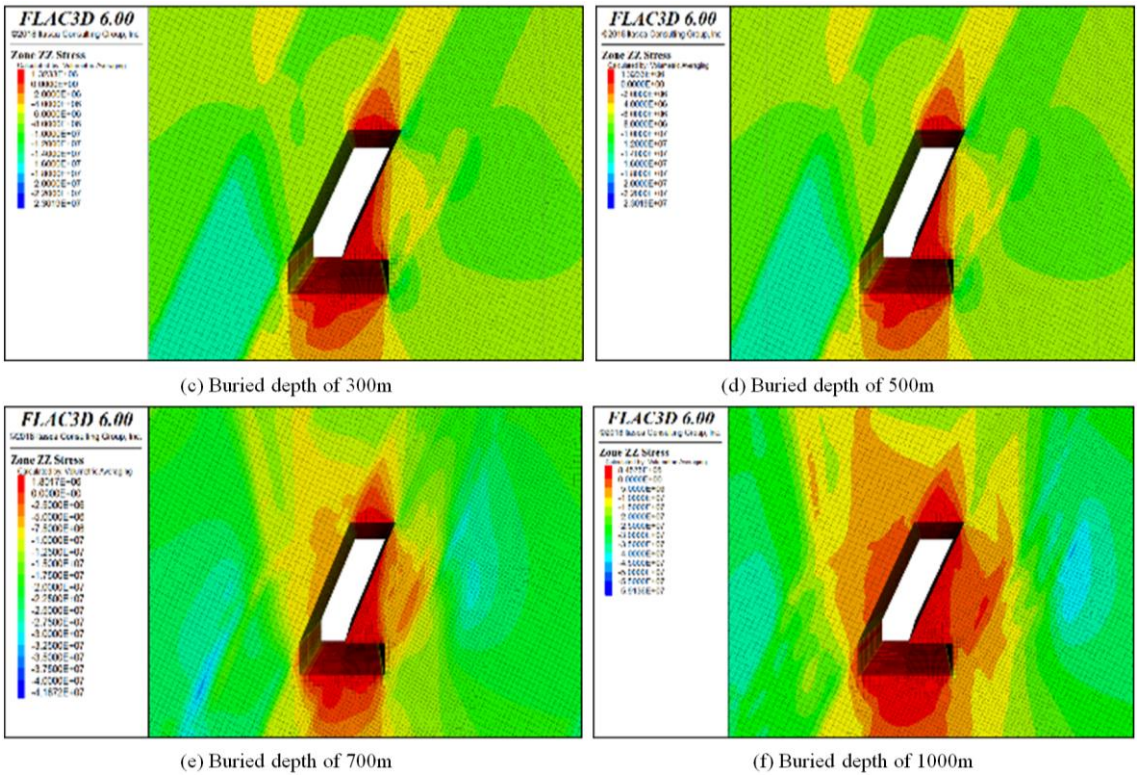

(c) Buried depth of 300m (d) Buried depth of 500m

(e) Buried depth of 700m (f) Buried depth of 1000m

Figure 4. *Vertical stress distribution in roadway surrounding rock post-advancement of the working face.*

3.2. Strain of Surrounding Rock of Single-side Roadway

Figure 5 displayed that the roadway's surrounding rock experiences varying degrees of deformation. The roof showed significant horizontal displacement, which intensified as it approached the goaf. In contrast, the roadway walls exhibited minimal horizontal displacement, with the upper section displaying a larger shift compared to the lower part.

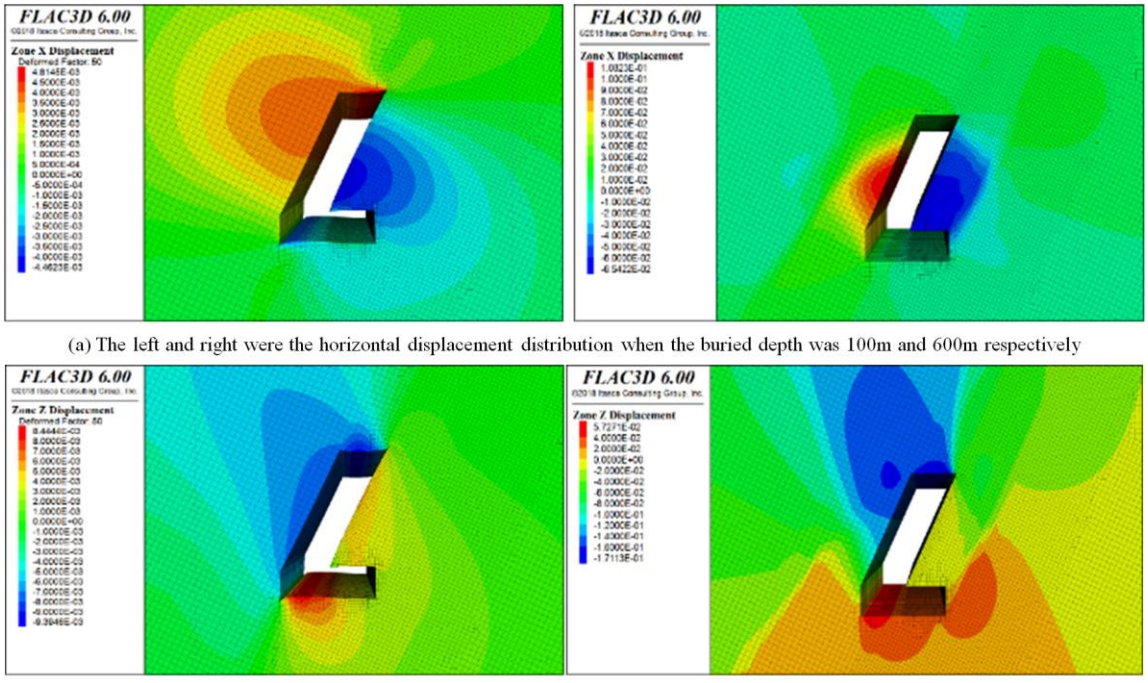

(a) The left and right were the horizontal displacement distribution when the buried depth was 100m and 600m respectively

(b) The left and right were vertical displacement distributions when the depth was 100m and 600m respectively

Figure 5. *Roadway displacement distribution following 100m burial depth advancement of the working face.*

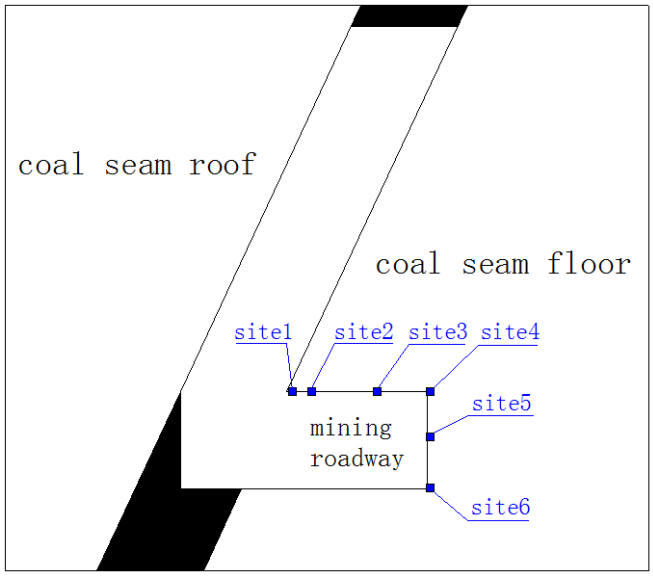

Figure 6. *Displacement measurement sites for roadway surrounding rock.*

Significant vertical displacement in the roadway primarily occurred at the roof, while minor bulging was observed on the floor due to the influence of the goaf. However, variations in vertical displacement of the surrounding rock at different burial depths were not immediately discernible from the diagram. To accurately assess these changes, displacement monitoring at six designated sites within the surrounding rock at varying burial depths was required. The positioning of these monitoring sites was illustrated in Figure 6, with horizontal displacement data provided in Table 2, and vertical displacement data presented in Table 3.

Table 2. *Horizontal displacements at monitoring sites for varying burial depths (unit: m).*

Depth/m	site1	site2	site3	site4	site5	site6
100	-0.003	-0.003	-0.004	-0.004	-0.003	-0.002
200	-0.006	-0.006	-0.007	-0.006	-0.005	-0.003
300	-0.016	-0.016	-0.017	-0.015	-0.008	-0.005
400	-0.029	-0.029	-0.029	-0.027	-0.018	-0.007
500	-0.047	-0.047	-0.047	-0.041	-0.022	-0.007
600	-0.065	-0.065	-0.064	-0.054	-0.031	-0.008
700	-0.091	-0.091	-0.090	-0.068	-0.038	-0.009
800	-0.127	-0.123	-0.122	-0.095	-0.053	-0.011
900	-0.167	-0.166	-0.164	-0.129	-0.076	-0.014
1000	-0.227	-0.223	-0.219	-0.177	-0.113	-0.019

Table 3. *Vertical displacements at monitoring sites for varying burial depths (unit: m).*

Depth/m	site1	site2	site3	site4	site5	site6
100	-0.001	0.002	0.004	0.003	0.002	0.002
200	0.004	-0.006	-0.008	-0.007	0.004	0.004
300	0.004	-0.006	-0.007	-0.006	-0.008	0.008
400	0.001	0.003	0.003	0.001	-0.005	0.012
500	-0.007	-0.005	-0.007	-0.008	0.004	0.016
600	-0.014	-0.012	-0.013	-0.010	0.005	0.019
700	-0.026	-0.024	-0.023	-0.010	0.005	0.022
800	-0.036	-0.036	-0.032	-0.013	0.0012	0.026
900	-0.047	-0.045	-0.044	-0.027	-0.006	0.030
1000	-0.061	-0.060	-0.060	-0.029	-0.013	0.035

Based on the monitoring data, a line chart was constructed to visually represent the movement of the surrounding rock in the roadway. Figure 7 and Figure 8 indicate that the trend of each line remains stable, with no significant fluctuations observed. Consequently, noticeable plastic deformation was evident in both the transverse and longitudinal directions.

As displayed in Figure 7, the displacement variation at each site exhibited an approximately parabolic trend with increasing tunnel depth. When the roadway was shallow, the surrounding rock experienced minimal stress, resulting in limited horizontal deformation and easier roadway maintenance. In contrast, at greater depths, the surrounding rock was subjected to significant stress, leading to substantial horizontal displacement and considerable difficulty in maintaining the roadway. Additionally, the roof displacement increased significantly at sites 1, 2, and 3 as the tunnel depth increased, while the horizontal displacement at sites 4, 5, and 6 on the roadway wall decreased progressively. Notably, at site 6, the horizontal displacement stabilized despite increasing depth. These observations indicate that the horizontal displacement at the roof exceeds that of the walls, and the farther the roof was from the walls, the more pronounced the displacement becomes, with a greater sensitivity to the depth of burial. Conversely, horizontal displacement diminished as the distance from the roof increases, although the influence of tunnel depth became more pronounced.

Figure 8 presented that as roadway burial depth increased, the vertical displacement of surrounding rock exhibited distinct patterns at various sites. Between depths of 100m and 400m, site 1 moved upward, while from 500m to 1000m, it shifted downward. Sites 2 and 3 demonstrated nearly identical vertical displacement across all burial depths. For depths

ranging from 100m to 400m, sites 2 and 3 showed subsidence in positive correlation with the upward movement of site 1. When the depth increased to 500m–1000m, the vertical displacement and trends of sites 1, 2, and 3 became nearly uniform. Between 100m and 500m, the displacement at site 4 closely aligned with that of sites 2 and 3. However, at depths of 600m–1000m, the subsidence trend at site 4 was noticeably restrained, mirroring the behavior of site 5, which also represented the third site of the roadway. Meanwhile, site 6 exhibited a consistent upward movement, attributed to the stress acting on the roadway floor.

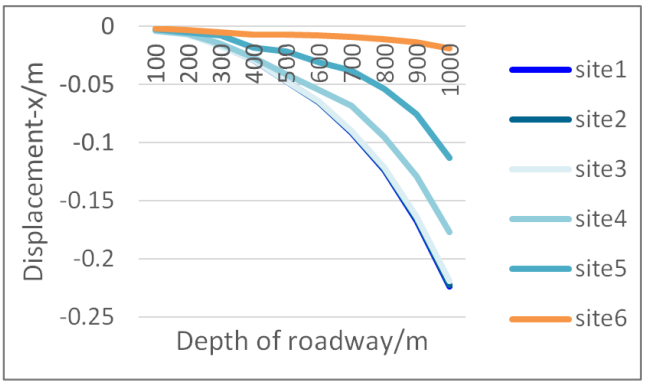

Figure 7. *Line graph of horizontal displacements at monitoring sites across varying burial depths.*

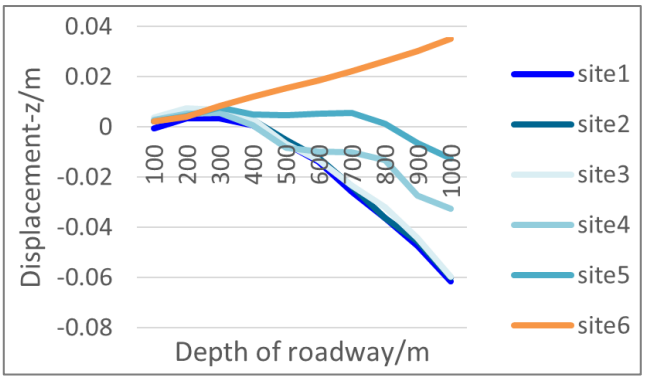

Figure 8. *Line graph of horizontal displacements at monitoring sites across varying burial depths.*

3.3. Comprehensive Stress-strain Analysis of Single-side Roadway

The stress distribution of the roof and walls of the roadway, analyzed through a combination of stress-strain behavior and rock mass stress, can be simplified for clarity. As depicted in Figure 9, the primary forces acting on the roof and walls were the gravitational load of the prominent "triangular" rock block and the internal stresses of the surrounding rock mass. As the roadway depth increased, the internal stress within the surrounding rock intensified, resulting in varying degrees of deformation.

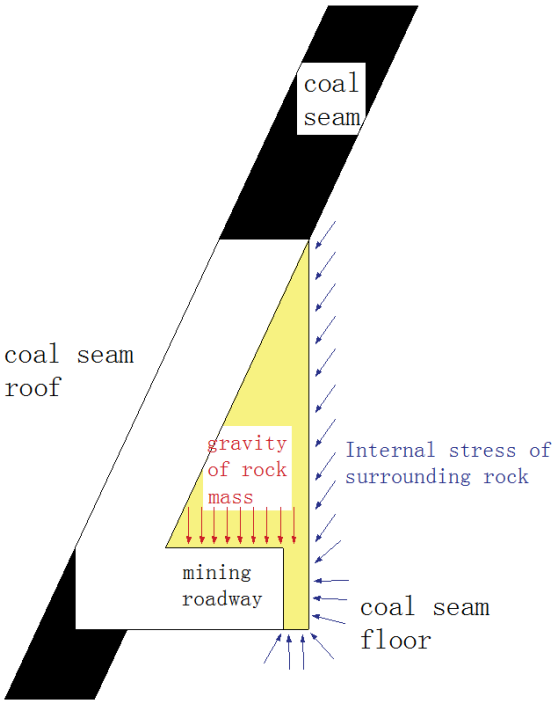

Figure 9. *Stress state schematic of rock block in the "triangle area".*

Analysis of the displacement charts revealed that the deformation patterns of the roadway surrounding rock can be categorized into three types based on varying burial depths. The first type, depicted in Figure 10, occurred at shallow depths around 100m, where significant pressure was observed on the roadway floor, accompanied by a slight overall rise in the roof, floor, and walls. The roof adjacent to the goaf exhibited minor subsidence due to gravitational forces and the bending moment exerted by the "triangular" rock mass. In the second type, illustrated in Figure 11, for burial depths between 200m and 400m, the internal stress within the surrounding rock intensified, resulting in general displacement toward the goaf. The combined influence of rock mass gravity and internal stress caused the roadway roof to exhibit a downward trend, though a slight increase was noted at the goaf-side roof end compared to the initial position. Lastly, as shown in Figure 12, for deeper burial depths ranging from 400m to 1000m, the increased internal stress became the dominant factor driving surrounding rock deformation. Notable displacement of the roof and walls toward the goaf occurred, with the upper wall exhibiting greater horizontal displacement than the lower portion. The wall near the roadway floor showed minimal horizontal movement, while the roof experienced subsidence. Additionally, the floor rose, and the walls entered a zone of vertical stress concentration, with significant compressive stress.

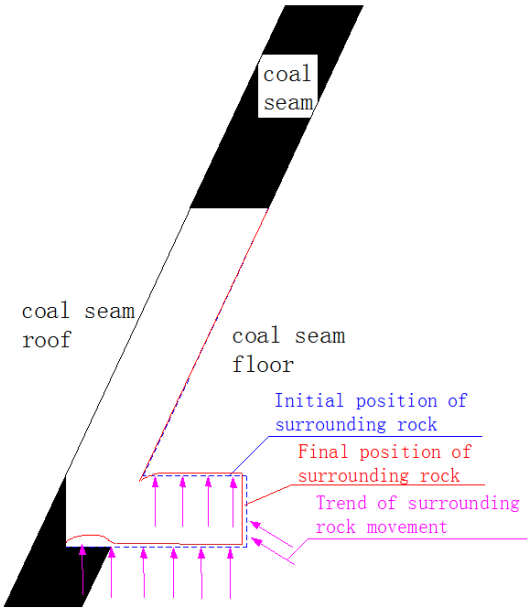

Figure 10. *Deformation trend of the surrounding rock in a single-side roadway at a buried depth of approximately 100m.*

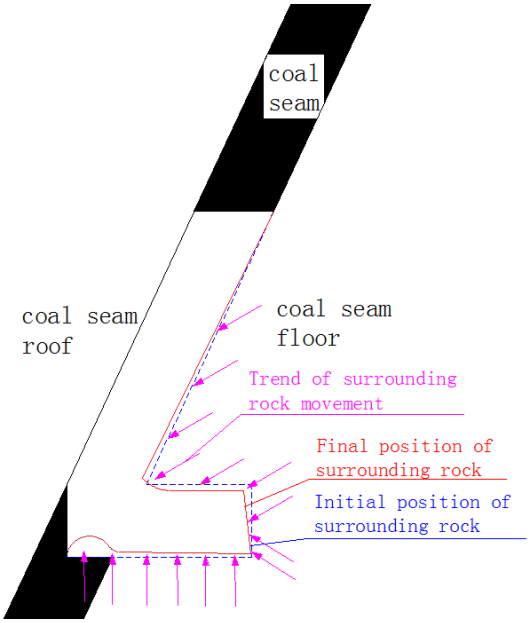

Figure 11. *Deformation trend for a buried depth ranging from 200m to 400m.*

For shallow burial depths (approximately 100m or less), the surrounding rock primarily experienced gravitational forces from the protruding "triangular" rock mass above the roadway. Consequently, roadway retention measures emphasized sealing off the gob and preventing wind channelling, with minimal focus on mitigating deformation. At moderate depths (200m to 400m), inadequate maintenance led to significant roof displacement, necessitating retention strategies aimed at resisting roof subsidence. At greater depths (400m to 1000m), increased subsidence occurred, with both the roof and the adjacent wall near the goaf showing considerable horizontal and vertical displacement. Thus, retention efforts focus on controlling roof subsidence and lateral movement.

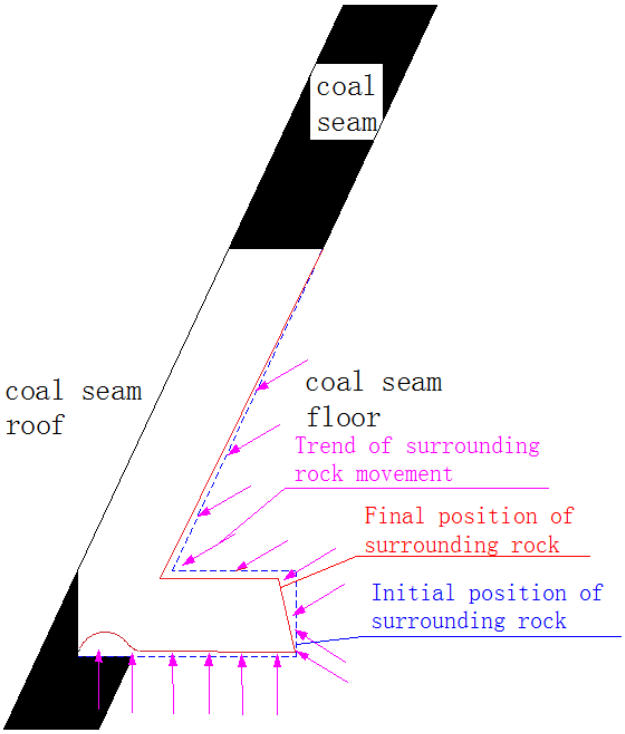

Figure 12. *Deformation trend of surrounding rock of single-side roadway with buried depth of 500m to 1000m.*

4. Roadway Support Method and Construction Technology

The design for the mining area of Mine 8 targeted coal seams at depths ranging from 50m to 400m, aligning the single roadway top coal caving method within the same depth range. Taking both technical and economic factors into account, no distinction was made in the retention support measures between roadways at depths below 100m and those between 100m and 400m.

4.1. Roadway Support Method Before the Advancing of the Working Face

To satisfy the operational requirements of the single roadway caving top coal mining method, a 3.8m-wide and 2.5m-high rock roadway was constructed on the coal seam floor. Roof support was implemented using a "cable bolt + anchor mesh" system. During excavation, temporary roof support was installed first, followed by the application of a metal mesh. Bolt holes were drilled according to the specified spacing, after which the bolts were installed and secured. Two anchor cables were positioned at an 85 ° angle to rein-

force roof stability, with additional anchor cables placed at regular intervals. For the roadway walls, support consisted of a combination of anchor rods, light steel belts, and metal mesh. The bolts were metal with a diameter of φ20 mm and a length of 2.5m, spaced at 700×800mm intervals. The anchor cables were 7.2m in length, with a spacing of 1400×1600mm. Details of the support system were illustrated in Figure 13.

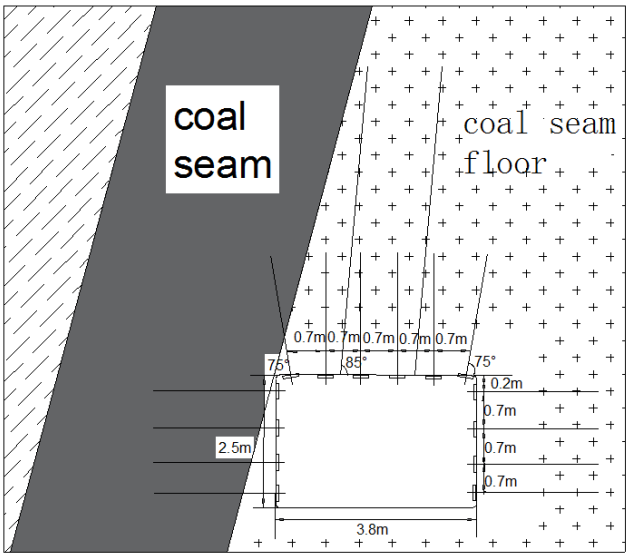

Figure 13. Schematic diagram of the initial support method of a single roadway.

4.2. Roadway Side Support Method

(1) The buried depth of the roadway was less than 100m

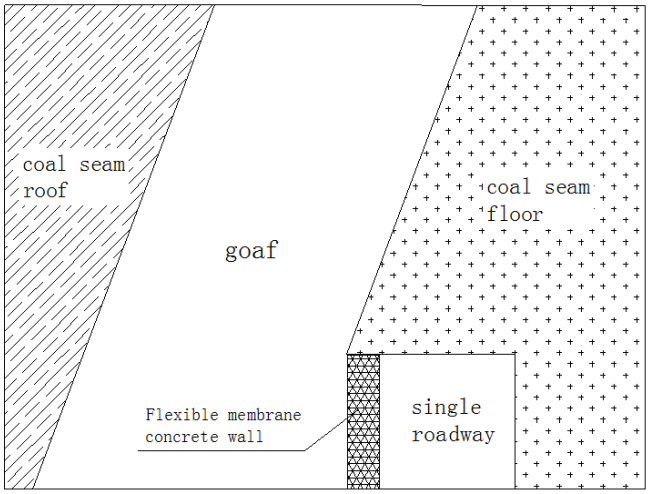

Figure 14. Schematic diagram of roadway side support mode for roadway with buried depth less than 100m.

At a burial depth of less than 100m, the influence of depth on the "single roadway" following the advancement of the working face was minimal. The "triangular" suspended rock mass above the roadway was effectively stabilized by the flexible concrete wall, which also isolated the goaf, as illustrated in Figure 14.

(2) Roadway with buried depth of 100m~400m

To mitigate roof subsidence and lateral roadway displacement, I-beam scaffolding was employed to reinforce the support after the flexographic concrete wall was poured. As depicted in Figure 15, the I-beam shed formed a right-angle trapezoid, effectively minimizing the displacement of the roadway side toward the goaf caused by the internal stress of the surrounding rock.

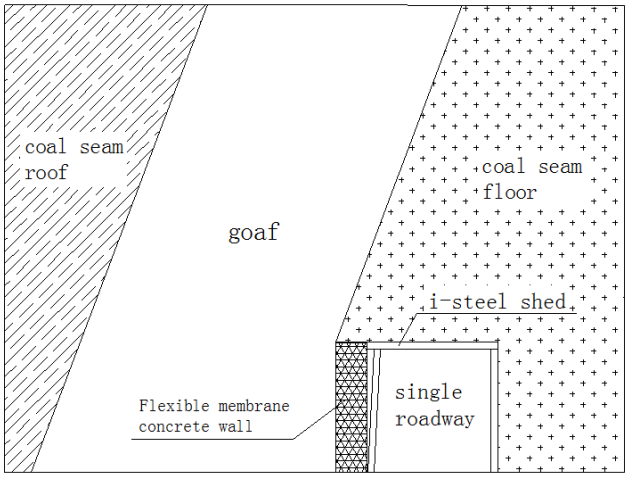

Figure 15. Schematic diagram of roadway side support mode with buried depth of 100m to 400m.

4.3. Construction Process of Retaining Roadway Support

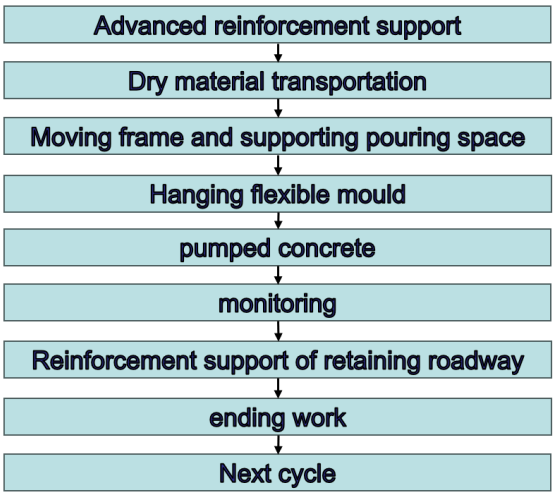

Figure 16. Schematic diagram of process flow.

The construction of flexible form pumping concrete along

the hollow retaining lane involves three critical aspects (e.g., [10]): space support for pouring, flexible formwork installation, and pumped concrete application, as illustrated in Figure 16. After the working face advances, temporary support must be promptly established for the pre-pouring space of the flexible form. At the end of the frame, three rows of single pillars, spaced 500mm×500mm, should be installed (e.g., [11]). These pillars supported a π-shaped steel beam against the roadway roof within the construction area of the concrete wall to mitigate roof deformation, as shown in Figure 17.

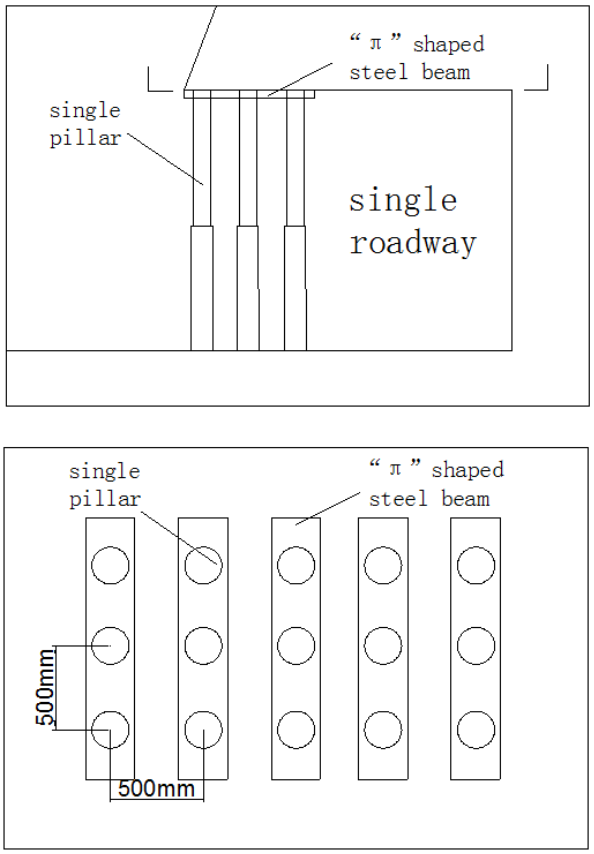

Figure 17. *Schematic diagram of temporary support in flexure preplacement space.*

To ensure a secure connection between the flexible formwork and the base, the bottom plate was leveled prior to the construction of the flexible form concrete wall. The construction process for the flexible form concrete wall followed these steps: a. Insert the steel bars, serving as the framework, into the sleeve of the top flange, and secure them to the flexible form flange using No. 10 galvanized iron wire; b. Employ a single hydraulic prop to stabilize the steel bars and the initial support's metal mesh against the roof, providing temporary roof support; c. Pump the prepared concrete into the flexible form until it adheres tightly to the roof; d. Utilize the permeable and non-permeable properties of the flexible form by refilling the form after ensuring no water seepage from the concrete. This process was repeated 3 to 4 times to guarantee a full connection of the concrete to the roof; e. Once the flexible concrete wall had cured for 3 to 5 days, reaching 70–80% of its final strength, the single hydraulic prop was removed (e.g., [12]).

For roadways with a burial depth of 100m to 400m, I-beam sheds should be installed to reinforce the support following the removal of the hydraulic prop.

5. Determine the Reasonable Width of the Flexographic Concrete Wall

5.1. Theoretical Calculation

(1) Flexographic concrete bearing capacity calculation

Drawing on the operational experience of similar mines and the specific conditions of the working face, a 1m-wide concrete wall was recommended for roadways at depths of less than 100m. For roadways at depths between 100m and 400m, a 1.2m-wide concrete wall was proposed. Theoretical calculations were now performed to assess the bearing capacity of the filling wall, which was dependent on the internal composition of structural materials. In this case, C30-grade concrete, known for its higher strength, was employed as the filling material for the flexible mold. The pull anchor bolt, acting as a "skeleton," exerts transverse binding forces on the concrete. The specified pull anchor bolts, φ24×1350, were arranged in rows of four, with a spacing of 800mm×1000mm between rows (e.g., [13]).

The bearing capacity (N_1) of the flexographic concrete was derived using the specified formula (e.g., [4])

$$N_1=\varphi(f_{cc}+4\sigma_r)\ A'_c \tag{1}$$

The binding σ of the anchorr was calculated by

$$\sigma_r = \frac{\sigma_b \pi d^2}{4a_1a_2} \tag{2}$$

Where, N_1 represented the bearing capacity of a C30 concrete wall (kN/m); φ denoted the stability coefficient, set at 0.97; σ_r was the effective binding force exerted on the bolt (MPa); A'_c referred to the section area of the concrete (m^2), with a value of 1.2m^2; f_{cc} was the compressive strength of C30 concrete, defined as 15.8 MPa; d indicated the diameter of the anchor bolt, specified as 20 mm; σ_b signified the tensile strength of the steel bar (MPa), with a value of 300 MPa; a_1 and a_2 represented the row spacing of the anchor bolt arrangement, measured at 800 mm × 1000 mm.

The effective binding force of the anchor bolt was calculated as σ=0.12 MPa, and the bearing capacities of the flexible concrete walls, with widths of 1.0 m and 1.2 m, were determined to be 15,791.6 kN/m and 18,949.9 kN/m, respectively.

(2) Flexographic concrete supporting load calculation

As the roadway roof was not part of the coal seam, the

load on the concrete wall cannot be calculated using the articulated rock block theory. Based on previous mechanical analyses, at a burial depth of 100m, the maximum bearing pressure on the flexible form concrete was limited to the weight of the overlying "triangular" rock block. Between 100m and 400m, the flexible form concrete also absorbs a portion of the internal pressure from the surrounding rock, though the predominant load remains the triangular rock block. When the bearing capacity of the flexible form concrete significantly exceeded the weight of the "triangular" rock block, the support conditions were satisfied, yielding the following inequality:

$$N_2 = \frac{(d+x)h\gamma f}{2} \ll N_1 \quad (3)$$

In the formula: N_2 represented the pressure per unit length on the flexible concrete wall (kN/m); d was the remaining roadway width (m); x was the width of the concrete wall (m); h denoted the mining height of the top coal caving (m); γ was the rock density, taken as 24 kN/m ³; f was the compensation coefficient, take 1.5.

Upon calculation N_2=1069.2kN/m. The load-bearing capacity of the flexible membrane concrete wall, with widths of 1.0m and 1.2m, significantly exceeded N_2, confirming its adequacy in meeting the engineering requirements.

5.2. Numerical Simulation Analysis of Flexure Concrete Bearing Capacity

Theoretical calculations and analysis indicated that a 1m-wide flexible film concrete wall was sufficient to meet safety production requirements at a buried depth of up to 100m, while a 1.2m-wide wall was necessary for depths between 100m and 400m. Following this analysis, FLAC3D numerical simulation software was used to evaluate the stress-strain behavior of the roadway under these two depth conditions.

(1) Model establishment

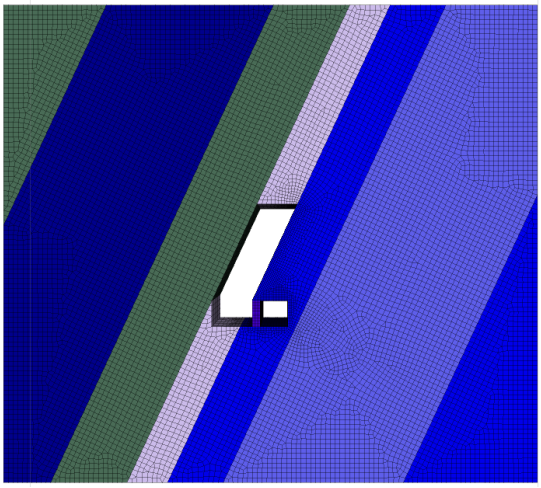

Figure 18. *FLAC3D modeling diagram of lane retention.*

Two models were constructed based on the surrounding rock conditions following the advancement of the original working face. In the first model, referred to as Model I, the buried depth was set at 100m, with a 1m-wide concrete wall added to the goaf side of the roadway. The second model, referred to as Model II, applies a buried depth of 400m and a 1.2m-wide concrete wall on the same side. The grid surrounding the roadway was refined for higher resolution, as illustrated in Figure 18, and the physical and mechanical properties of the rock strata were listed in.

(2) Numerical simulation analysis

Parameters were assigned to each rock layer and concrete wall, followed by the application of initial ground stress. The resulting horizontal stress distribution for the roadway and concrete wall was illustrated in Figure 19. The figure demonstrated that, under the influence of the flexible film concrete wall, horizontal stress concentrations developed in the roadway roof at burial depths of 100m and 400m. The flexible film concrete wall effectively resisted the roof's tendency to shift toward the goaf and endures substantial shear stress.

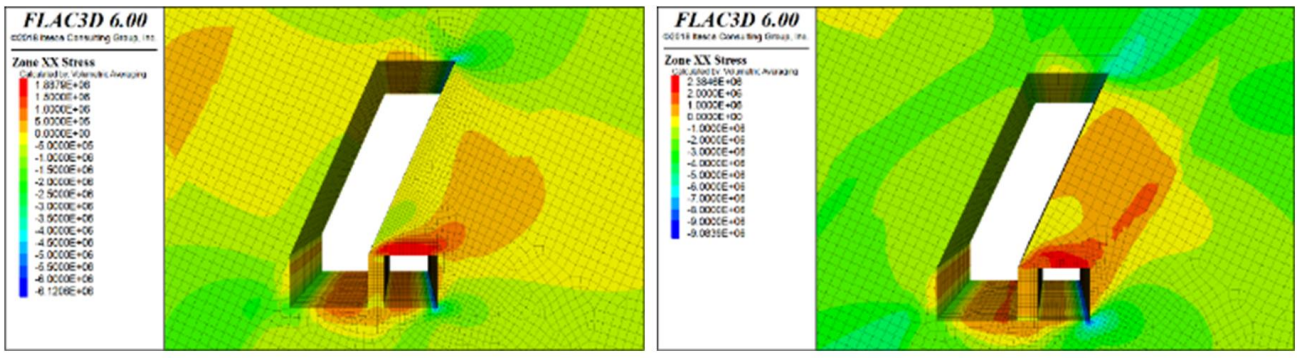

(a) Model1 (b) Model 2

Figure 19. *Horizontal stress distribution of roadway surrounding rock.*

As shown in Figure 20, the simulated vertical stress distribution of the roadway and concrete wall revealed that, following mining, the vertical force exerted on the original roadway roof closer to the goaf shifts. The stress concentration on the roadway roof adjacent to the goaf, caused by the overlying rock mass, was alleviated after the concrete wall was installed.

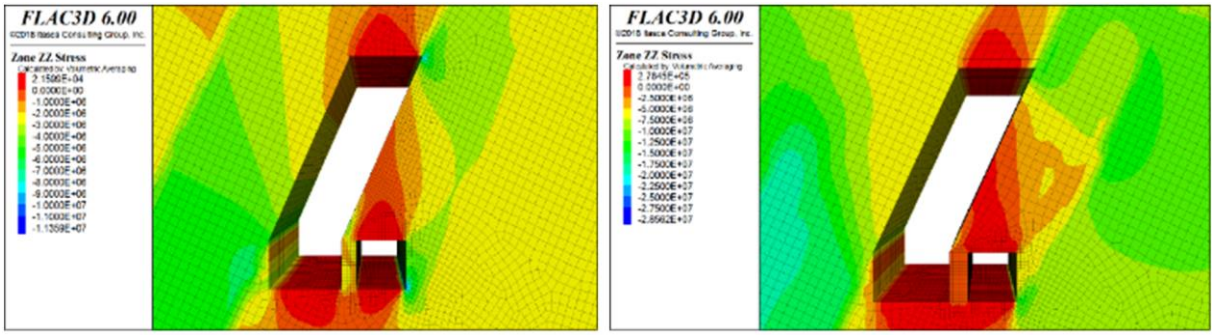

(a) Model 1 (b) Model 2

Figure 20. *Vertical stress distribution of roadway surrounding rock.*

Figure 21 and Figure 22 displayed the horizontal and vertical stress distributions in the surrounding rock of the roadway, revealing significant plastic deformation in both models. When the roadway was maintained using a concrete wall, the roof movement slows considerably, though the wall was subjected to shear and compressive stresses from above. With a burial depth of 100m and a 1m-wide flexible membrane concrete wall, the maximum horizontal displacement was 11mm, and roof subsidence remains under 20mm, indicating minimal displacement. At a depth of 400m, with a 1.2m-wide flexible mold concrete wall, horizontal displacement increases to 54mm, and roof subsidence reaches 90mm, indicating substantial movement. Consequently, an auxiliary support system using right-angle trapezoidal I-beam sheds was recommended for this roadway retention method.

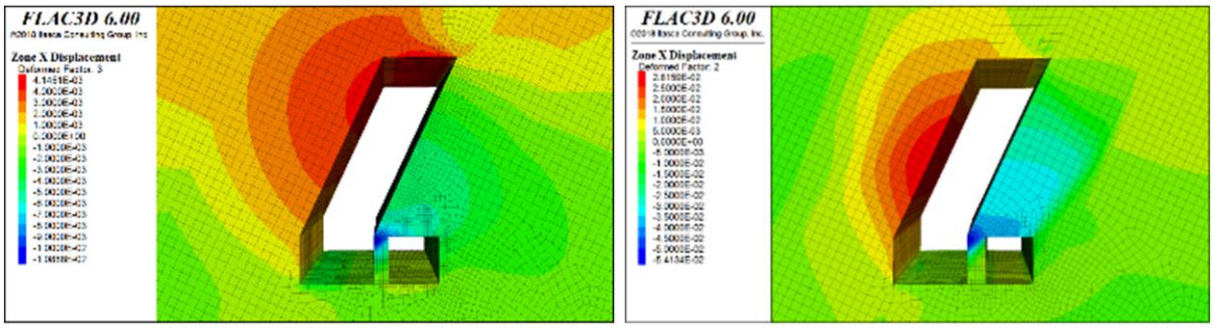

(a) Model1 (b) Model 2

Figure 21. *Horizontal stress distribution of roadway surrounding rock.*

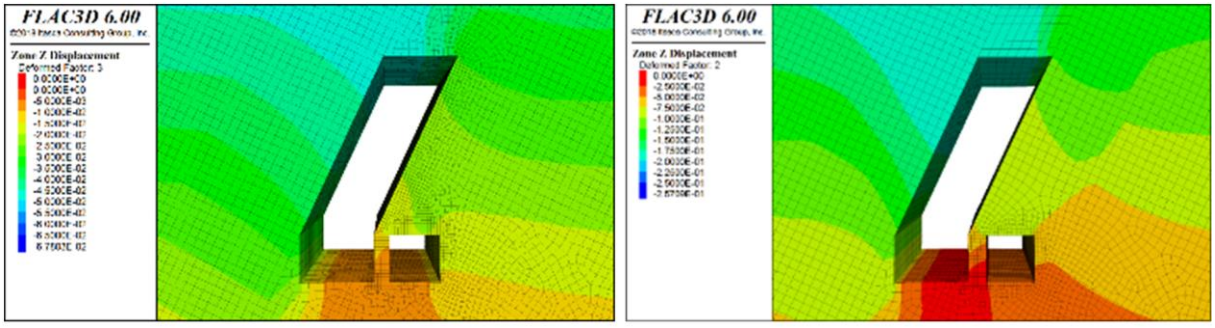

(a) Model 1 (b) Model 2

Figure 22. *Horizontal stress distribution of roadway surrounding rock Vertical stress distribution of roadway surrounding rock.*

In conclusion, the FLAC3D numerical simulation demonstrated that maintaining roadway stability in steep single rock roadways can be effectively achieved using a 1m-wide flexible mold concrete wall for roadways at a depth of 100m, and a 1.2m-wide wall for those at a depth of 400m. For roadways buried at 400m, the installation of a right-angle trapezoidal I-beam support structure played a significant role in controlling deformation and further stabilizing the roadway.

6. Conclusions

(1) Based on the geological conditions of the No. 8 coal seam in a specific mine, the stress-strain behavior of the surrounding rock in a single-side roadway following the advance of the working face is investigated, employing the top coal caving method for single-side roadways. The study reveals distinct movement patterns of the surrounding rock at different depths: shallow (100m), intermediate (100m to 400m), and deep (400m to 800m). These observations offer a foundation for further research on roadway retention in similar mining environments.

(2) For roadways buried below 100m, a single roadway retention method along the goaf is recommended through the construction of a flexible concrete wall. For depths between 100m and 400m, the proposed method includes building a flexible form concrete wall in conjunction with a right-angle trapezoid I-beam support. Theoretical calculations and numerical simulations confirm the feasibility of both methods. These approaches enable the formation of full negative pressure ventilation at the working face, effectively isolating the goaf, preventing gas accumulation and spontaneous combustion of residual coal, and ensuring a safer working environment for miners.

(3) The "steeply inclined medium-thick layer single roadway top coal mining method" is designed for steeply inclined medium-thick coal seams with significant variations in seam thickness, dip angle, and complex geological conditions. However, this method results in complex stress conditions in the surrounding rock of the roadway, and the lack of comprehensive theoretical support for roadway retention highlights the need for further research to strengthen the theoretical framework.

Abbreviations

Top-caving	Top Coal Caving

Author Contributions

Kangzhan Ding: Formal Analysis, Investigation, Validation, Writing – original draft

Zhaowen Du: Conceptualization, Writing – review & editing

Zongbin Ma: Supervision

Jiandu Su: Data curation

Zhongping Guo: Resources

Funding

This work is not supported by any external funding.

Data Availability Statement

The data is available from the corresponding author upon reasonable request.

Conflicts of Interest

The authors declare no conflicts of interest.

References

[1] Manchao He, Shangyuan Chen, Zhibiao Guo, et al. Control of surrounding rock structure for gob-side entry retaining by cutting roof to release pressure and its engineering application, Journal of China University of Mining & Technology, 2017, 46-48(5), 959-969. https://link.oversea.cnki.net/doi/10.13247/j.cnki.jcumt.000696

[2] Xiaoqing Wang. Mechanism of pressure relief by advanced pre-splitting in gob-side entry retaining and arrangement principle of pre-splitting boreholes, Journal of Mining & Safety Engineering. 2024, 1-13. https://doi.org/10.13545/j.cnki.jmse

[3] Qi Wu, Yongjian Zhu, Heng Ren. On key parameter of gob-side entry retaining under the condition of inclined thick layer and hard roof, Journal of Hunan University of Science and Technology (Natural Science Edition). 2023, 38(4), 1-11. https://link.oversea.cnki.net/doi/10.13582/j.cnki.1672-9102.2023.04.001

[4] Haijun Guo, Huailong Du. Research and application of flexible formwork concrete gob-side entry retaining technology in thick coal seam, Coal Science and Technology. 2022, 50(S2), 105-112. https://link.oversea.cnki.net/doi/10.13199/j.cnki.cst.2022-1961

[5] Zifei Zhang, Anmin He. Analysis of surrounding support and stability on gob-side entry retaining with flexible-formwork concrete in shallow seam, Coal Science and Technology. 2013, 9(9), 24-28. https://link.oversea.cnki.net/doi/10.13199/j.cnki.cst.2013.09.009

[6] Tingjun He. Application of Wilson hinged rock Block Theory to roadway side support design, Chinese Journal of Rock Mechanics and Engineering. 1998(02), 63-67.

[7] Henghu Sun, Jian Wu, Yunxin Qiu. Rules of ground pressure and strata control in gateways maintained in goaf, Journal of China Coal Society. 1992(01), 15-24.

[8] Min Tu. Study on Roof movement and side support resistance of goaf Retaining Roadway, Journal of Liaoning Technical University (Natural Science). 1999, (04), 347-351.

[9] Kangzhan Ding, Zhongping Guo, Zongbin Ma, et al. Research and application of single roadway top caving mining method in steep dip medium thick coal seam, Coal Technology. 2024, 43(02), 67-70. https://link.oversea.cnki.net/doi/10.13301/j.cnki.ct.2024.02.014

[10] Ruiyun Tian. Practice of goal-side entry retaining in fully mechanized coal mining face with medium thick coal seam in Shendong Mining Area, Coal Science and Technology. 2015, 43(S2), 9-13.

[11] Zizheng Zhang, Jianbiao Bai, Xiangyu Wang, et al. Practice of gob-side entry retaining in fully mechanized coal mining face with medium thick coal seam in Shendong Mining Area, Coal Science and Technology. 2023, 48(11), 3979-4000. https://link.oversea.cnki.net/doi/10.13225/j.cnki.jccs.2023.0382

[12] Weiqi Yuan, Jun Zhuo, Ying Shen. Matchingf equipment and construction technology of flexible concrete gob-side roadway protectionin inclined coal seam, Coal Technology. 2020, 39(04), 40-43. https://link.oversea.cnki.net/doi/10.13301/j.cnki.ct.2020.04.011

[13] Xiaobai Li, Haibing Pan, Jingshuai Shi, et al. Study on road-side support technology of 6m high cutting working face, Coal Engineering. 2019, 51(05), 78-81.

Biography

Kangzhan Ding is a master student at the School of Energy and Mining Engineering, Shandong University of Science and Technology, under the supervision of Professor Guo Zhongping. Participated in the research and report writing of a number of horizontal topics, mainly focusing on the mining of steeply inclined coal seam, trying to solve the difficult problem of steeply inclined coal seam mining.

Research Fields

Kangzhan Ding: teep coal seam mining, green mining technology, roadway support technology, roadway retention technique along goaf, Mining method optimization

Zhaowen Du: mining damage and environmental protection, paste filling mining, new solid waste filling material modification, steep coal seam mining, green mining technology

Zongbin Ma: steep coal seam mining, green mining technology, mine disaster prediction and prevention, roadway surrounding rock control, mining method optimization

Jiandu Su: steep coal seam mining, green mining technology, roadway support technology, mine disaster prediction, roadway surrounding rock control

Zongping Guo: green mining technology, mine disaster prediction and prevention, mine roadway support, steep coal seam mining, rock burst prevention